



Effects of Range Requirements and Battery Technology on Electric VTOL Sizing and Operational Performance

Matthew M. Warren*, Andrea Garbo*, Mark T. Kotwicz Hemiczek*, Thomas K. Hamilton*, and Brian J. German†

Georgia Institute of Aerospace Engineering, Atlanta, GA, 30332, U.S.A

In this paper, we explore how range and battery technology factors such as specific energy and maximum C-ratings affect the sizing and performance of electric VTOL (eVTOL) aircraft operating in the context of Urban Air Mobility (UAM) missions. The approach leverages a simple aircraft performance model of sufficient abstraction to be suitable for a wide range of potential eVTOL configurations including lift plus cruise, quadcopter, and side-by-side helicopter configurations. Using this performance model, we examine sizing and performance of a presumed UAM network in the greater San Francisco area. The output from this model is used to determine the optimal size of the aircraft with respect to factors such as the number of flights completed and profitability. The optimal weight for maximizing the number of completed routes can be determined analytically and is the weight at which both the charger power and the allowable charge C-rate are maximized unless the aircraft must be larger to fly the sizing mission. The profitability is also determined analytically and follows trends similar to the optimal weight for routes completed. Finally, we explore sensitivities of profitability and routes completed to changes in specific energy, charger power, and charge C-rate. Increasing specific energy always increases profitability while charger power and charge C-rate must be increased together.

Nomenclature		
B_c	discharge cycles to battery replacement	$P_{ch}^{(max)}$ maximum charging power
C_{ch}	charging C-rate	P_{cr} cruise power
D_A	available discharge	P_h hover power
D_R	discount rate (yearly), %	P_{Ind} landing power
\dot{C}_c	discharge C-rate	P_{res} res power
E_b	battery energy	Q total capacity discharged, Ah
E_c	average energy consumption per trip, kWh/trip	Q_n total capacity discharged at linearization point, Ah
E_{tot}	total energy used during flight	R internal resistance, Ω
η_{el}	electrical efficiency	R economic range, mi
FOM	Figure Of Merit	U battery voltage, V
G	dependency of voltage on depth of discharge and current, $\Omega/(Ah)$	U_0 no load battery voltage, V
I_{CC}	initial capital cost, \$	U_n battery voltage at linearization point, V
I_R	hull insurance rate (yearly), %	V_{vc} vertical climb rate at takeoff
i	current, A	V_{cr} cruise speed
K	dependency of voltage on capacity discharged, V	$V_{i,h}$ hover induced velocity
$(L/D)_e$	equivalent Lift-Drag ratio	\dot{h} cruise climb rate
L_F	average vehicle load factor	W_G vehicle weight, lbs
M_R	maintenance rate (yearly), %	W_p payload weight
N_{cr}	average number of completed routes per day	c_0 annual fixed costs, \$/year
\tilde{N}_{cr}	number of completed routes per unit time	c_1 annual weight-varying costs, \$/year
N_P	aircraft passenger capacity	c_2 energy-varying costs, \$/kWh
P_{vc}	vertical climb power	c_3 revenue per trip, \$/trip
P_{cc}	cruise climb power	ω_{batt} battery derating factor
P_{ch}	charging power	t_{vc} vertical climb time during takeoff
		t_{vc} vertical descent time during landing
		t_{ch} charging time

*Graduate Research Assistant, School of Aerospace Engineering, 270 Ferst Drive, and AIAA Student Member.

†Langley Associate Professor, School of Aerospace Engineering, 270 Ferst Drive, and AIAA Associate Fellow.

t_{mis}	mission time	ϕ_p	payload weight fraction
t_{res}	reserve time	ρ_E	energy density
t_{tot}	total time	$\$_B$	base ticket price, \$
t_h	hover time	$\$_{\text{BAT}}$	battery replacement cost, \$
$\Pi^{(\max)}$	maximum profit per day, \$	$\$_E$	cost of electricity, \$/kWh
Π	profitability index, \$ per day	$\$_T$	ticket price, \$
ϕ_b	battery weight fraction	$\$_V$	variable ticket price, \$/mi
ϕ_e	empty weight fraction		

I. Introduction

There has been a dramatic upsurge in interest in an envisioned passenger travel mode in cities commonly referred to as Urban Air Mobility (UAM). An initial vision for UAM involves 4-6 passenger vertical takeoff and landing (VTOL) aircraft with electric propulsion and high degrees of autonomy that operate in a point-to-point network of “vertiports” within metropolitan areas. Based on recent and projected advancements in battery specific energy, these electric VTOL (eVTOL) aircraft are anticipated to become feasible in the near term for short flights of 20-50 miles. Uber has committed to developing an eVTOL UAM network in the Dallas/Fort Worth area and has plans to expand to other cities in the future [1].

This paper explores eVTOL UAM by investigating relationships between aircraft mission performance, battery technology factors, and economics. The performance metrics of interest are the number of missions the aircraft can complete in a fixed period of time including battery recharge time, the energy expended, and the potential for profitability. The technology factors examined include maximum charge and discharge C-rate, battery specific energy, and charger power. The primary purpose of the paper is to assess optimal sizing of eVTOL aircraft based on differences in the maximum range requirement and in the demand-weighted average flight distance, i.e. the economic range, in a UAM network. Because of the severe limitations on aircraft performance resulting from current levels of battery specific energy, small differences in these UAM mission requirements associated with city-to-city variations in these factors are anticipated to have a first-order effect on the technical feasibility and economic viability of an eVTOL UAM service. The performance of the aircraft is computed using a high level of abstraction model of a mission in the greater San Francisco area using the methodology presented in [2].

II. Modeling

Aircraft performance in UAM networks is estimated using a high-level model appropriate for requirements analysis and early conceptual design studies. We model a full mission profile including vertical flight and forward flight phases as well as a complete reserve mission to appropriately account for the implications of hover and reserve on battery energy requirements. Vertical flight performance (hover and vertical climb) is computed with actuator disk theory based on representative disk loadings and figures of merit associated with different vehicle types. Forward flight performance is modeled based on estimates of vehicle weight and equivalent lift-to-drag ratio at associated nominal airspeeds. Battery performance is modeled with an “energy in a tank” model with appropriate derating factors based on battery cell manufacturer data sheets as shown in Section II.A.

We present a sizing approach to determine weight for an aircraft that must meet a specified maximum range constraint and operate repeated trips at a specified economic range in a way that maximizes profitability. The sizing approach incorporates a constraint on maximum discharge C-rate. Additionally, a simple economic model (Section II.B) is presented to allow the effects of aircraft size and battery parameters to be investigated.

It is important to point out a few notes about the methodology used to generate our results. The high level of abstraction increases the applicability of the model but renders the aircraft model very sensitive to the input values. The battery model requires a choice of battery derating factors which are only valid near the weight for which they were selected. Any numbers presented for profitability are difficult to obtain and substantiate due to a lack of data. For these reasons, the paper is explained such that the reader can draw their own conclusions or replicate the results with a different set of inputs. Additional work has been completed on determining the ideal flight speed for operating an aircraft in a UAM network which could be used to generate input parameters [3].

Lastly, an example case is presented which walks through all of the values used throughout the analysis portion (Section V) of the paper.

A. Battery Modeling

A number of approaches can be taken toward battery modeling depending on the required level of fidelity. In this work, the aircraft performance model is formulated at a high-level and pairs nicely with a similarly simple battery model that might best be described as an “energy in a tank” model. This type of model assumes that there is a fixed amount of total energy that can be drawn from the battery, similar to a gas tank, and models the total available battery energy as the product of a fixed specific energy and the battery mass. The amount of battery energy remaining is therefore simply the initial energy minus the energy expended in flight. Unfortunately, the assumptions of the model neglect a key dependency of the discharge rate on the battery capacity. In reality, the amount of energy that can be provided by the battery to the load decreases as the discharge rate increases. Environmental factors such as temperature and usage related factors such as the number of cycles accrued by the battery and calendar age also have important effects.

Our approach uses a battery derating factor which we apply to the total battery energy to model the capacity-reducing influence of several important operational factors while maintaining overall model simplicity. To estimate the derating factor, we modeled the battery cell performance using a discharge model based on a regression of cell discharge data. The resulting derating factor was then applied to adjust the specific energy used in the “energy in a tank” representation in our aircraft performance model.

The model, shown in Eq. (1), considers voltage as a function of current and depth of discharge. The model accounts for effects on voltage due to state of charge and discharge current. The values of U_0 , K , R , and G can be determined from a least-squares-fit of a digitized battery discharge plot over a range of battery state-of-charge values in which the voltage drop is nearly linear for lithium ion batteries, e.g. 95% to 15%.

$$U = U_0 - KQ - Ri - GiQ \quad (1)$$

For performance analysis, propeller driven airplanes and helicopters generally fly in (approximately) constant power mission segments. The total amount of energy expended during a flight segment with constant power for a given time is simply $\Delta E = Pt$. The relationship, $P = iU$, can be substituted into the initial battery curve fit to eliminate current and express the relationship in terms of power.

$$U = U_0 - KQ - RP/U - GQP/U \quad (2)$$

Whereas the original model is linear with respect to discharge capacity, Q , substituting for power results in a model nonlinear with respect to Q . It is therefore convenient and sufficiently accurate to linearize the resulting equation. The Taylor series expansions of $1/U$ and Q/U are shown below where U_n and Q_n represent the values of voltage and discharge capacity, respectively, about which the function is linearized.

$$\frac{1}{U} = \frac{1}{U_n} - \frac{1}{U_n^2}(U - U_n) \quad (3)$$

$$\frac{Q}{U} = \frac{Q_n}{U_n} - \frac{Q_n}{U_n^2}(U - U_n) - \frac{1}{U_n}(Q - Q_n) \quad (4)$$

These linearized expressions are then substituted into Eq. (2) which is then simplified resulting in:

$$U = U_n - \tilde{K}(Q - Q_n) \quad (5)$$

where,

$$U_n = \frac{1}{2}((U_0 - KQ_n) + \sqrt{(U_0 - KQ_n)^2 - 4(RP_G P Q_n)}) \quad (6)$$

$$\tilde{K} = \frac{K + GP/U_n}{1 - RP/U_n^2 - GPQ_n/U_n^2} \quad (7)$$

To obtain the energy withdrawn from the battery by the load, Eq. (5) must be integrated using the relation $dE = UdQ$. The integral of this expression is:

$$\Delta E_{12} = \frac{1}{2}(U_1 + U_2)(Q_2 - Q_1) \quad (8)$$

where,

$$U_1 = U_n - \tilde{K}(Q_1 - Q_n) \quad (9)$$

$$U_2 = U_n - \tilde{K}(Q_2 - Q_n) \quad (10)$$

Eq. (8) can be arranged to determine the final state of charge, Q_2 , which results from extracting a specified energy from the battery at an initial state of charge, Q_1 .

$$Q_2 = Q_1 - \frac{2\Delta E_{12}}{U_1 + U_2} \quad (11)$$

B. Economic Modeling

A simplified, rough order of magnitude (ROM) economic model has been developed to estimate the effects of eVTOL aircraft characteristics on the profitability potential of UAM operators. The daily profitability potential per aircraft, termed the *profitability index* (Π), is defined as the difference between daily revenue and costs per aircraft as shown in Eq. (12).

$$\Pi = \text{daily revenue per aircraft} - \text{daily costs per aircraft} \quad (12)$$

The profitability index can be expanded into Eq. (13) by modeling the daily revenue as a function of the number of completed routes per day (N_{cr}) and by grouping costs into three categories: energy-dependent costs, gross-weight dependent costs, and size-independent costs, each of which is multiplied by a constant. Energy costs vary as a function of the number of completed routes per day and the average energy consumption per trip (E_c), while weight varying costs are only a function of the vehicle weight (W_G), and size-independent costs are represented by the constant c_0 .

$$\Pi = c_3 N_{cr} - (c_2 N_{cr} E_c + \frac{c_1}{365} W_G + \frac{c_0}{365}) \quad (13)$$

The revenue constant (c_3) represents the profitability of each completed trip and can be further expanded to consider the ticket price ($\$T$) and average number of passengers per flight ($N_P L_F$) to obtain Eq. (14):

$$c_3 = \$T N_P L_F \quad (14)$$

where the ticket price ($\$T$) is the sum of a fixed base ($\$B$) and distance-dependent rate ($\$V$), as shown in Eq. (15).

$$\$T = \$B + \$V R \quad (15)$$

The energy-based cost constant (c_2) denominates the overall cost of operation per kWh and can be expanded to consider the electricity rate ($\$E$) used for battery charging, the cost of battery replacement ($\$B$) and the battery replacement rate (B_c) to obtain Eq. (16):

$$c_2 = \$E + \frac{\$_{BAT}}{B_c} \quad (16)$$

where it should be noted that the term $\$_{BAT}/B_c$ has units of $\$/\text{kWh}$ due to the term B_c effectively being unitless and can therefore be summed with $\$E$. Lastly, making the assumption that the acquisition cost of the vehicle (I_{CC}) is a function of its weight [4], the weight-based cost constant (c_1), can be expanded to consider the annual acquisition ($I_{CC} D_R$), hull insurance ($I_R I_R$), and maintenance costs ($I_{CC} M_R$) as demonstrated in Eq. (17).

$$c_1 = \frac{I_{CC}}{W_G} (D_R + I_R + M_R) \quad (17)$$

where D_R , I_R , and M_R represent the annual discount rate, hull insurance rate, and maintenance rate, respectively. The size-independent cost constant (c_0) is not expanded here but is included to consider costs such as the pilot's salary. Rewriting Eq. (13) with the expanded coefficient definitions, the profitability index can be expressed as Eq. (18)

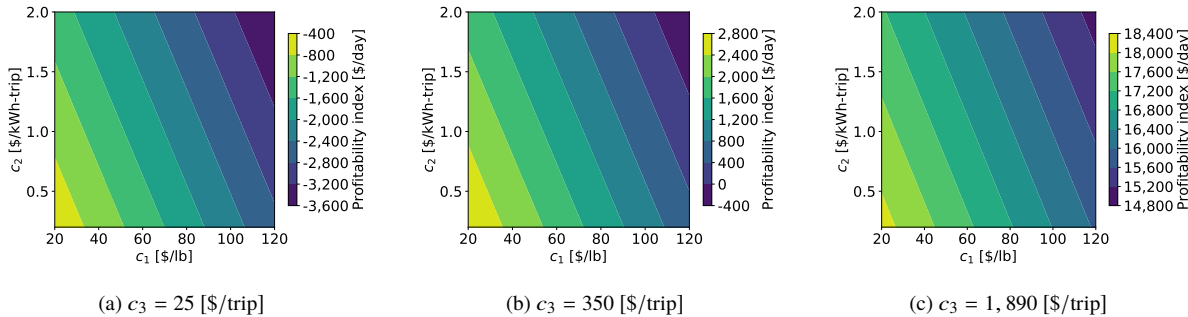
$$\Pi = \$T N_P L_F N_{cr} - \left[N_{cr} E_c \left(\$E + \frac{\$_{BAT}}{B_c} \right) + \frac{I_{CC}}{365} (D_R + I_R + M_R) + \frac{c_0}{365} \right] \quad (18)$$

Example low, mid-range, and high values for c_1 , c_2 , and c_3 , adapted in part from Refs. [4–6], are given in Table 1, where the sensitivity of each coefficient to its component parameters is made clear. As such, the above formulas are better suited for a ROM sensitivity analysis and care should be taken when using the above formulas to obtain any dollar values.

Table 1 Example values for economic coefficients c_1 , c_2 and c_3 ($R = 20$ mi).

Value	I_{CC}/W_G	D_R	$I_R + M_R$	c_1	$\$_E$	$\$_{BAT}$	B_c	c_2	$\$_B$	$\$_V$	N_P	L_F	c_3
Low	200	5%	5%	20	0.05	200	3,000	0.12	5	1	2	50%	25
Mid	300	10%	10%	60	0.1	350	1,000	0.45	25	5	4	70%	350
High	400	15%	15%	120	0.3	500	300	1.97	50	15	6	90%	1,890

The design space for the simplified economics model described by Eq. (13) using the above coefficients is illustrated in Fig. 1 to further demonstrate the importance of the appropriate selection of each coefficient. It should be noted that the sensitivity analysis on profitability presented in Section V uses the non-expanded form of c_1 and c_2 , and assumes a fixed cost of \$80,000 for c_0 (also used in Fig. 1), representative of a typical pilot salary. Different values for c_0 are not considered since relative rather than absolute results are of interest with regards to the economic model in this paper.

**Fig. 1 Simplified economic model design space ($W_G = 8,000$ lbs, $N_{cr} = 10$, $E_c = 50$ kWh).**

C. Network Modeling

In the high level of abstraction used in the models described in this study, two parameters are required to define a city UAM network. A maximum range is required for the sizing mission and represents the furthest distance the aircraft would ever be expected to fly without recharging. The second parameter is the economic range which is defined as the demand-weighted mean mission distance. The economic mission length is assumed to be much shorter than the maximum distance and is used in the assessment of profitability. The maximum range requirement for an eVTOL UAM aircraft would presumably be based on the total percentage of a local market that an operator desires to capture, and the economic range is determined by the distribution of demand for origin-destination pairs in a defined vertiport network. Both range values could be determined, in principle, by UAM studies such as those performed by German, et al. [2, 7] which develop demand distributions. An example demand distribution for commuting trips based on Longitudinal Employer-Household Dynamics Origin-Destination Employment Statistics (LODES) data for the San Francisco area is shown in Fig. 2. The 50th percentile trip distance is the economic range, and the 90th percentile might be the basis for the maximum range requirement.

The sizing mission definition used in this paper is a simplified variant of [8] and is shown in Table 2 and Section II.C. The simplified includes takeoff, landing, cruise, and reserve and neglects shorter transient flight periods such as transition flights. Range credit for descent is not presumed. Off-design missions do not include the reserve segment.

D. Aircraft Performance

Aircraft performance is analyzed in an energy based fashion where the total energy required to complete the mission (E_{tot}) is the sum of the energy required during each mission segment divided by η_{el} to take in consideration electrical system efficiency (Eq. (19)). The energy consumed during each phase of the mission is simply the duration of that phase multiplied by the power required by the aircraft in that operative condition.

$$E_{tot} = \frac{1}{\eta_{el}} \sum_i P_i t_i \quad (19)$$

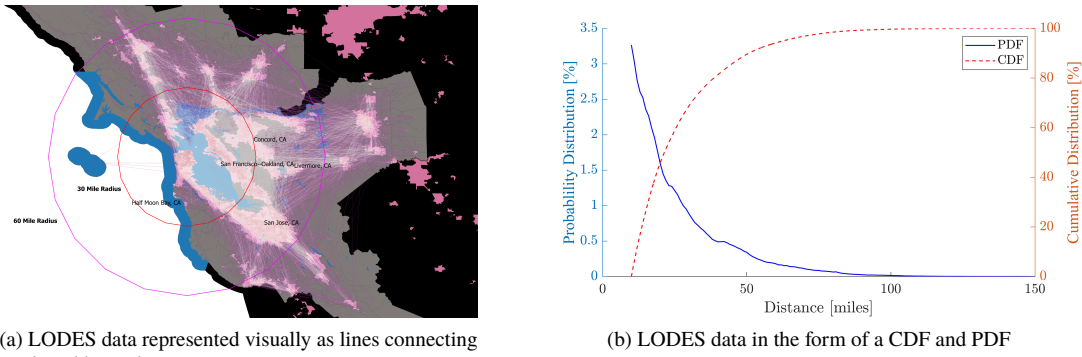


Fig. 2 Greater San Francisco LODES data representations.

Table 2 Segments in design mission.

Parameter	S1	S2	S3	S4	S5	S6	S7
Segment	Takeoff	Hover	Cruise Climb	Cruise	Hover	Land	Reserve Cruise
Type	Vertical	Vertical	Horizontal	Horizontal	Vertical	Vertical	Horizontal
Climb rate (fpm)	100	0	900	0	0	0	0
Altitude (ft)	6,000	6,000	10,000	10,000	6,000	6,000	10,000
Duration	30 sec	10 sec	until alt. target	mission distance	30 sec	30 sec	20 min

As illustrated in Eqs. (20) and (24), those power values are function of aircraft takeoff weight (W), mission requirements, and some other parameters used to described the aircraft performance on each particular operative condition. Vertical flight is modeled using actuator disk theory which requires estimates of disk loading (σ) and figure of merit (FOM), leading to the definition of hover induced velocity ($V_{i,h}$) in Eq. (20), power required in hover (P_h), and power required in vertical climb (P_{vc}) in Eq. (22).

$$V_{i,h} = \sqrt{\frac{\sigma}{2\rho}} \quad (20)$$

$$P_h = W \frac{V_{i,h}}{\text{FOM}} \quad (21)$$

$$P_{vc} = W \frac{V_{i,h}}{\text{FOM}} \left(\frac{V_{vc}}{2V_{i,h}} + \sqrt{\left(\frac{V_{vc}}{2V_{i,h}} \right)^2 + 1} \right) \quad (22)$$

Forward flight segments are modeled with an equivalent lift to drag ratio, $(L/D)_e$, which can be used to compare the performance of both helicopters and airplanes, leading to the equations for power required during cruise (P_{cr}) in Eq. (23),



Fig. 3 Visualization of design mission.

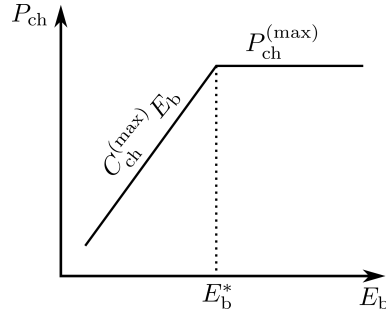


Fig. 4 Maximum charge power as a function of energy density.

and during cruise climb (P_{cc}) in Eq. (24) (where V_{cr} stands for cruise speed and \dot{h} for cruise climb rate).

$$P_{\text{cr}} = W \frac{V_{\text{cr}}}{(L/D)_e} \quad (23)$$

$$P_{\text{cc}} = W \left(\frac{V_{\text{cr}}}{(L/D)_e} + \dot{h} \right) \quad (24)$$

The power required during reserve and landing segments (P_{res} and P_{Ind}) are assumed equal to P_{cr} and P_h , respectively. All descents are considered no credit descents so it is not necessary to model descending flight in either forward or vertical flight.

The total energy available is equal to the energy stored in the battery and calculated as:

$$E_b = W \omega_{\text{batt}} \rho_E (1 - \phi_e - \phi_p) \quad (25)$$

where ρ_E is the battery energy density, ω_{batt} is the battery energy derating factor, and ϕ_e and ϕ_p are the empty and payload weight fractions, respectively. To scale the aircraft up and down, ϕ_e remains fixed along with W_p . Increases in gross weight cause ϕ_p to decrease, leading to increases in ϕ_b , W_b and E_b . The amount of energy required to return the battery to a fully charged state is assumed to be exactly equal to the energy discharged from the battery during flight (Eq. (19)). Additionally, we model battery charging assuming a constant power charge that is limited both by the maximum allowable charging C-rate ($C_{\text{ch}}^{(\text{max})}$) of the battery and the maximum allowable power of the charger:

$$P_{\text{ch}} = \min \left(P_{\text{ch}}^{(\text{max})}, C_{\text{ch}}^{(\text{max})} E_b \right) \quad (26)$$

where $P_{\text{ch}}^{(\text{max})}$ is the maximum power provided at the charging station. An example of P_{ch} as functions of E_b is shown in Fig. 4 where the E_b at which the charge rate ceases to be limited by C-rate and begins to be limited by $P_{\text{ch}}^{(\text{max})}$ is denoted $E_b^* = P_{\text{ch}}^{(\text{max})} / C_{\text{ch}}^{(\text{max})}$.

Combining Eq. (19) with the Eqs. (21) to (24), and rearranging the terms, E_{tot} can be written as

$$E_{\text{tot}} = W \tilde{R} \quad (27)$$

where the \tilde{R} coefficients has dimensions of a distance. The three \tilde{R} used later in the performance analysis are defined as follows

$$\tilde{R}^{(1)} = \frac{1}{\eta_{\text{el}}} (P_{\text{vc}} + P_h (t_{h,1} + t_{h,2} + t_{vd}) + \Delta h) \quad (28)$$

$$\tilde{R}^{(\text{F})} = \tilde{R}^{(1)} + \frac{1}{\eta_{\text{el}}} \frac{R}{(L/D)_e} \quad (29)$$

$$\tilde{R}^{(\text{R})} = \tilde{R}^{(\text{F})} + \frac{1}{\eta_{\text{el}}} \frac{V_{\text{cr}} t_{\text{res}}}{(L/D)_e} \quad (30)$$

where Δh is the altitude change during the cruise climb phase.

1. Maximum Range

The maximum range $R^{(\max)}$ is obtained by equating the energy required to complete a mission, including the reserve segment, with the energy available in the battery.

$$W\tilde{R}^{(R)} = \omega_{\text{batt}}E_b \quad (31)$$

Substituting Eqs. (25) and (30) in Eq. (31) and solving for R , it is possible to obtain the equation for the maximum range, $R^{(\max)}$, that a given aircraft with a particular battery technology can fly:

$$R^{(\max)} = \eta_{\text{el}}(L/D)_e \left(D_A \frac{E_b}{W} - \tilde{R}^{(1)} \right) - V_{\text{cr}} t_{\text{res}} \quad (32)$$

The contour plot of $R^{(\max)}$ as a function of W and ρ_E for the lift-plus-cruise configuration shown Table 3 flying the mission shown in Table 2 is reported in Fig. 5a. The white region in the plot represents the designs that are not able to reach the mission $R^{(\max)}$ requirement which, for this example, is set to 20 mi. As expected, the $R^{(\max)}$ can be improved by increasing the E_b by either increasing the size of the aircraft (W) or improving the battery technology (ρ_E).

2. Number of Completed Routes

Assuming that the aircraft is continuously operated, the number of routes completed in a unit time (\tilde{N}_{cr}) is

$$\tilde{N}_{\text{cr}} = \frac{1}{t_{\text{tot}}} \quad (33)$$

$$t_{\text{tot}} = t_{\text{mis}} + t_{\text{ch}} \quad (34)$$

where t_{tot} is the total time required to complete the mission (t_{mis}) and to recharge the battery (t_{ch}). Assuming that the energy used to complete the mission, without taking into consideration the reserve segment, is completely recharged at the end of each flight, the charging time is

$$t_{\text{ch}} = \frac{E_{\text{tot}}}{P_{\text{ch}}} \quad (35)$$

$$= \frac{W\tilde{R}^{(F)}}{\min(P_{\text{ch}}^{(\max)}, C_{\text{ch}}^{(\max)}E_b)} \quad (36)$$

Therefore, combining Eq. (33) and Eq. (36), \tilde{N}_{cr} can be written as:

$$\tilde{N}_{\text{cr}} = \left(t_{\text{mis}} + \frac{W\tilde{R}^{(F)}}{\min(P_{\text{ch}}^{(\max)}, C_{\text{ch}}^{(\max)}E_b)} \right)^{-1} \quad (37)$$

The contour plot of \tilde{N}_{cr} for the same example considered in Fig. 5a with a $C_{\text{ch}}^{(\max)} = 1.5$ [1/hr] and $P_{\text{ch}}^{(\max)} = 300$ [kW] is shown in Fig. 5b.

3. Profitability Index

Eq. (37) can be combined with Eq. (13) to obtain the Π for a particular aircraft configuration flying the design mission as a function of W and battery technology variables such as ρ_E , $P_{\text{ch}}^{(\max)}$ and $C_{\text{ch}}^{(\max)}$. An example contour plot for Π is presented in Fig. 5c.

III. Optimal Weight

It is clear from Figs. 5b and 5c that for a particular value of ρ_E , there exists a corresponding value of W which maximizes either \tilde{N}_{cr} or Π . A similar behavior is observed as other variables are considered. The objective of this section is to analytically derive equations for W which maximize \tilde{N}_{cr} and Π ($W^{(\tilde{N}_{\text{cr}})}$ and $W^{(\Pi)}$, respectively). By considering these optimal values, it is possible to reduce the dimensionality of the problem and show the optimal weight results as a function of battery technology parameters.

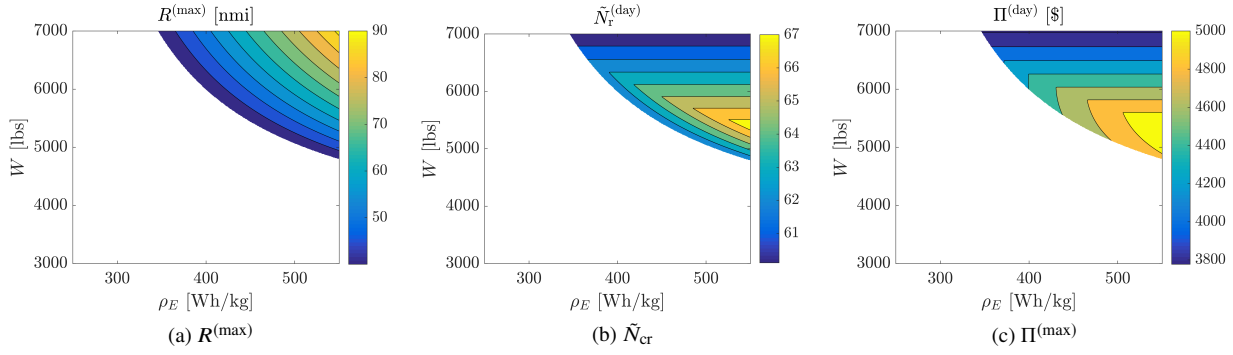


Fig. 5 Example of $R^{(\max)}$, \tilde{N}_{cr} and $\Pi^{(\max)}$ as function of W and ρ_E computed using economic model values described in Section IV, $P_{\text{ch}}^{(\max)} = 300$ [kW] and $C_{\text{ch}}^{(\max)} = 1.5$ [1/hr]

A. Optimal Weight for Maximizing Number of Completed Routes

Fig. 6a shows the same results as Fig. 5b with the addition of a curve (labeled as $W^{(\tilde{N}_{\text{cr}})}$) representing the values of W , which maximize the number of completed routes for the particular aircraft configuration as a function of ρ_E . Similar plots can be obtained as functions of the other design variables. As shown, this maximizing condition follows one of two different lines. It follows the maximum value of either the minimum W to satisfy the range condition (labeled as $W^{(R_{\max})}$), which is simply the lower boundary of the plot, or the W which maximizes Eq. (37) (labeled as $W^{(E_b^*)}$).

Differentiating Eq. (37) and solving $d\tilde{N}_{\text{cr}}/dW = 0$ shows that this condition occurs at the value of W such that E_b is equal to E_b^* in Fig. 4. More specifically, combining $E_b^* = P_{\text{ch}}^{(\max)}/C_{\text{ch}}^{(\max)}$ with Eq. (25), it is possible to obtain

$$W^{(E_b^*)} = \frac{1}{1 - \phi_e} \left(\frac{P_{\text{ch}}^{(\max)}}{C_{\text{ch}}^{(\max)} \rho_E} + W_p \right) \quad (38)$$

Therefore, $W^{(\tilde{N}_{\text{cr}})}$ can be found as:

$$W^{(\tilde{N}_{\text{cr}})} = \max \left(W^{(E_b^*)}, W^{(R_{\max})} \right) \quad (39)$$

and the maximum of N_{cr} is

$$N_{\text{cr}}^{(\max)} = \left(t_{\text{mis}} + \frac{W \tilde{R}^{(\text{F})}}{P_{\text{ch}}^{(\max)}} \right)^{-1} \quad (40)$$

B. Optimal Weight for Maximizing Profit

As was the case in Section III.A above, Fig. 6b shows the same results as Fig. 5c with the addition of a curve (labeled as $W^{(\Pi)}$) representing the values of W which maximize Π for the particular aircraft configuration as a function of ρ_E . Similar plots can be obtained as function of the other design variables.

As before, the lower bound for $W^{(\Pi)}$ is represented by $W^{(R_{\max})}$ which is a function of the maximum range sizing mission. Aircraft sized to weights below this curve cannot complete the sizing mission. The green and blue portions of the curve are obtained by solving $d\Pi/dW = 0$ using Eqs. (13) and (37). The min operator in the equation for \tilde{N}_{cr} (Eq. (37)) leads to two distinct conditions and therefore to two different solutions for $d\Pi/dW = 0$. In particular, the solution for $E_b \geq E_b^*$ corresponds to $W^{(E_b^*)}$ (Eq. (38)), while for $E_b < E_b^*$ (and therefore $P_{\text{ch}} = C_{\text{ch}}^{(\max)} E_b$) the solution is:

$$W^{(\Pi_{E_b})} = \frac{-L_1 - \sqrt{L_1^2 - 4L_2 L_0}}{2L_2} \quad (41)$$

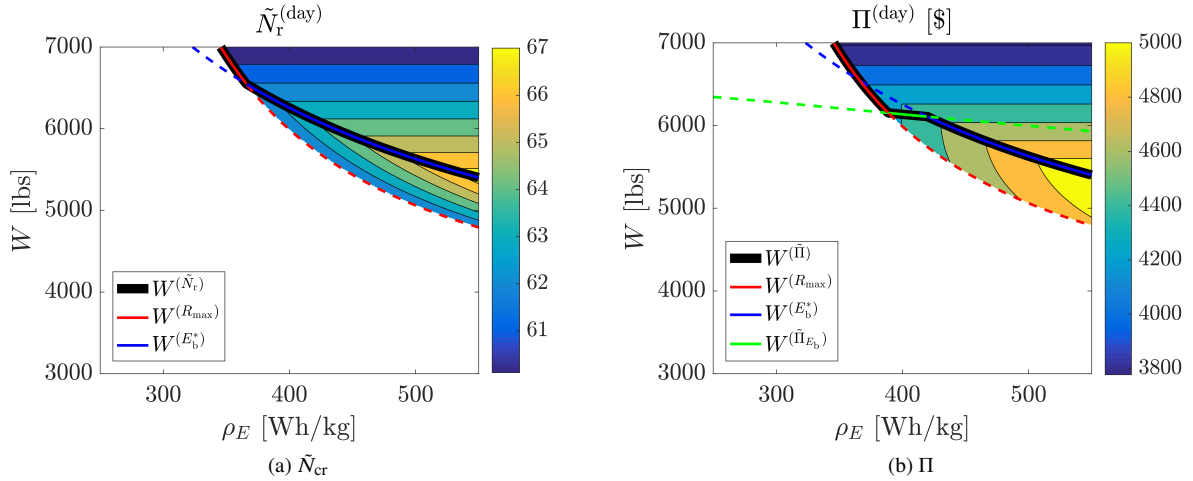


Fig. 6 Example of \tilde{N}_{cr} and Π as function of W and ρ_E with overlaid optimal W lines

where

$$L_0 = -c_1 k_4^2 - \tilde{R}^{(\text{F})} c_2 k_2 k_4 + c_3 k_5 \quad (42)$$

$$L_1 = 2k_4 \left(c_1 k_3 + \tilde{R}^{(\text{F})} c_2 k_1 \right) \quad (43)$$

$$L_2 = -c_1 k_3^2 - \tilde{R}^{(\text{F})} c_2 k_1 k_3 \quad (44)$$

$$k_1 = C_{\text{ch}}^{(\text{max})} \rho_E (1 - \phi_e) \quad (45)$$

$$k_2 = W_p C_{\text{ch}}^{(\text{max})} \rho_E \quad (46)$$

$$k_3 = t_{\text{mis}} C_{\text{ch}}^{(\text{max})} \rho_E (1 - \phi_e) + \tilde{R}^{(\text{F})} \quad (47)$$

$$k_4 = t_{\text{mis}} C_{\text{ch}}^{(\text{max})} \rho_E W_p \quad (48)$$

$$k_5 = k_2 k_3 - k_1 k_4 \quad (49)$$

Therefore, $W^{(\Pi)}$ can be found as:

$$W^{(\Pi)} = \max \left(W^{(R_{\text{max}})}, \min \left(W^{(\Pi_{E_b})}, W^{(E_b^*)} \right) \right) \quad (50)$$

IV. Example Problem

This section provides details about the variable values used to generate the results reported in the next section (Section V) and walks through the full process of generating those values.

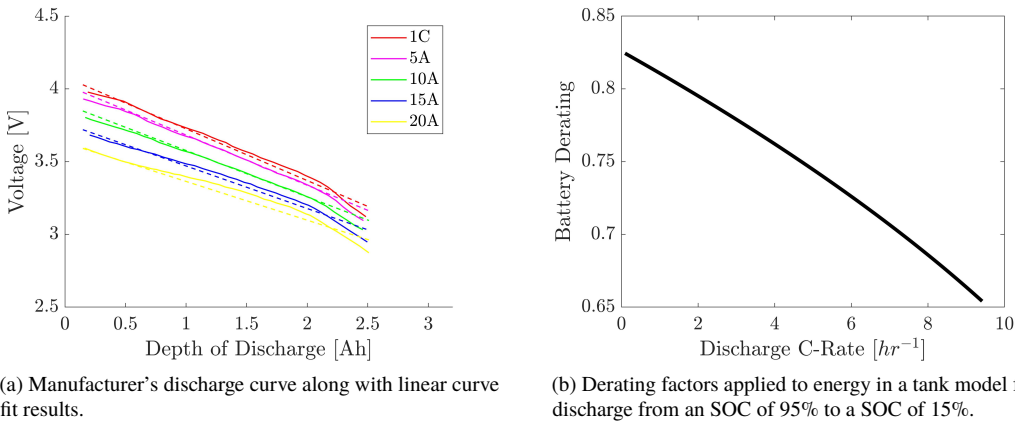
The sizing mission requires flying the full mission profile (Table 2) with reserve and with a cruise range equal to the maximum range of the aircraft ($\tilde{R}^{(\text{R})}$), while the economical mission is considered as the average mission flown by the aircraft. Under normal circumstances the aircraft does not fly the reserve segment in the economic mission, so reserve is excluded and the cruise distance is shortened to the economical range. For this example, our values for the maximum and economical range are 50 miles and 20 miles, respectively.

Aircraft performance inputs are shown in Table 3 and are based on the aircraft configurations presented by Silva and Johnson in [8]. These aircraft were chosen to represent the predicted performance of three general classes of aircraft and that demonstrate trade-offs on $(L/D)_e$, ϕ_e , and DL . These parameters are all that are necessary to complete the analysis due to the high level of abstraction maintained in modeling. The model assumes that the aircraft cruises only at V_{cr} for both the main cruise and reserve mission segments. The aircraft modeling does not involve full power required vs. flight speed profile implying that it is essential for the $(L/D)_e$ and V_{cr} to be appropriately matched. It is also important to note that all of these values are in typically quoted units and conversion to fundamental consistent units is necessary before use in the equations presented in Section II.D.

Table 3 Vehicle parameters.

Parameter	Quad	Side by Side	Lift plus Cruise
η	0.915	0.915	0.955
<i>FOM</i>	0.70	0.68	0.74
<i>DL</i> (lb/ft ²)	3.0	3.5	13.1
$(L/D)_e$	5.8	7.2	8.5
V_{cr} (kts)	98	98	112
W_{nom} (lb)	6,480	4,897	8,210
W_p (lb)	1,200	1,200	1,200
ϕ_e	0.571	0.549	0.648

The example battery cell chosen for this analysis is the Samsung INR18650-30Q which was the cell used in the NASA X-57 [9]. Using the battery model described in Section II.A results in the curve fit shown in Fig. 7. The manufacturer's discharge curve is digitized and the coefficients are determined from a least-squares-fit of the data. The model shows good agreement for the majority of the discharge curve (95% SOC to 15% SOC) and exhibits the largest deviation at high discharge values. During standard operations, it is assumed the battery is not charged above 95% to improve battery life. The battery is never allowed to be discharged below 15%, even for the reserve mission, to ensure performance is consistent and because lower voltages require higher currents to maintain a consistent power resulting in a possible runaway. The R-squared value for the curve fit shown is 0.985 for all the curves. Once the battery has been appropriately modeled, the integrated version of the battery model Eq. (11) was used to determine the battery derate (ω_{batt}) as a function of discharge C-rate as shown in Fig. 7. The total amount of energy available for flight is modeled as the nominal energetic capacity multiplied by the derating factor.

**Fig. 7** Battery discharge modeling.

Discharge C-rate varies with every stage of the flight as shown in Fig. 8; however, to maintain consistency with the level of abstraction of our performance model, a single derating factor is chosen based on the mission time average discharge C-rate (black solid line on Fig. 8). The C-rate is calculated by dividing the power that must be delivered by the battery for a mission segment by the nominal battery energy. In general, the C-rate required for each mission segment depends on the aircraft weight. Considering the average values of discharge C-rate in Fig. 8, and the battery derating factor (ω_{batt}) in Fig. 7, the estimated values for ω_{batt} range between 0.78 and 0.81, leading us to reasonably assume a fixed value of 0.8 for ω_{batt} .

Considering the battery and performance models described in the previous sections, the battery pack energy density (ρ_E), the maximum charging C-rate ($C_{ch}^{(max)}$), and the maximum power available at the charging station ($P_{ch}^{(max)}$) are the variables that define the battery and charging network technology. Those variables are the ones used in this study to

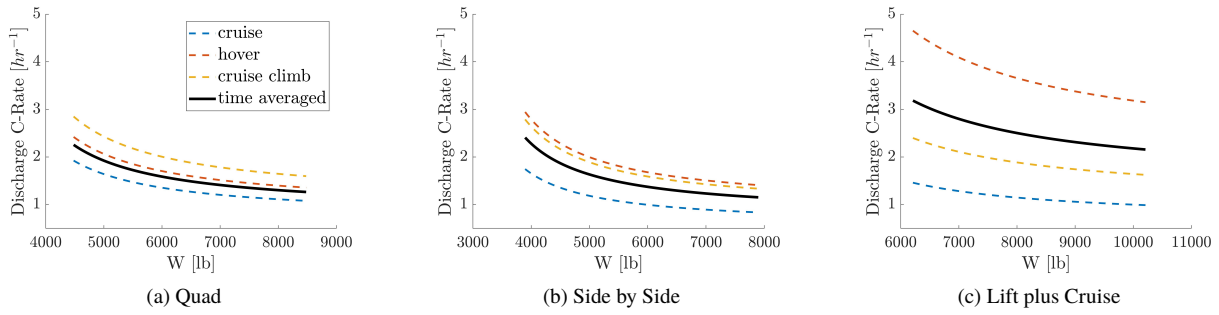


Fig. 8 Discharge C-rate for each flight segment.

define the design space where we conducted a performance sensitivity analysis of the different aircraft configurations flying the given mission. Based on battery datasheets for Samsung INR18650-30Q [10] and Panasonic NCR18650 [11], and publicly available information about existing or planned charging stations (Tesla [12], ABB [13], and Uber [1]), we decided to bound those technology variables as indicated in Table 4.

The economic constants (c_0 , c_1 , c_2 , and c_3) adopted to compute the profitability index (Eq. (13)) are shown in Table 5.

Table 4 Bounds for ρ_E , $C_{ch}^{(max)}$ and $P_{ch}^{(max)}$.

Variable	UB	LB
ρ_E [Wh/kg]	250	550
$C_{ch}^{(max)}$ [1/hr]	1	5
$P_{ch}^{(max)}$ [kW]	200	600

Table 5 Coefficient values used to characterize the economic model.

Coefficient	Value
$\$_B$ (fixed ticket price)	0.4 \$
$\$_V$ (variable ticket price)	1.55 \$/nmi
L_F (load factor)	0.75
c_0 (fixed cost)	80,000 \$/yr
c_1 (weight-varying cost)	70 \$/lbs/yr
c_2 (energy cost)	0.5 \$/kWh

V. Results and Sensitivities

This section shows the results in terms of profitability per day obtained by continuous repeated routes flown at the economic range for aircraft configurations sized to $W_G = W^{(II)}$ (Eq. (50)). The results are based on the mission provided in Table 2, and are presented as a function of the charger and battery technology parameters ρ_E , $C_{ch}^{(max)}$, and $P_{ch}^{(max)}$. In this results section, we also show how the influence of battery and charger technology on profitability and number of completed routes can be used to guide the aircraft sizing process, and to also inform research as to which technologies need further development in order to improve aircraft performance.

The profitability index is formulated as the revenue minus costs (Eq. (13)) where it is underlined how the most significant drivers of both revenue and cost are the number of completed routes per unit time (N_{cr}) and the weight (W_G) of the aircraft. As described in Section II.D, N_{cr} and W_G are primarily influenced by the aircraft configuration design – which can usually be chosen by the operator – and battery and charger technology parameters, which instead are typically constrained in their values.

Fig. 9 shows the contour plots of profitability index with respect to the charge C-rate and the battery specific energy at different maximum charger powers with overlaid the gradient arrows. First of all, an increase in the specific energy of the battery always leads to an increase in profitability mainly caused by the reduction in the aircraft weight (as confirmed in Fig. 12) required to fly the sizing mission, and therefore to weight related costs. A decreased aircraft weight also reduces the energy consumed during flight leading to a shortening in charge time (Eq. (36)), and consequentially to an increase in the number of completed routes and revenue.

The second observation is about the effect of technology improvement in the profitability index, as indicated by the gradient arrow direction and magnitude. For example, at low charger powers (Fig. 9a), an increase in maximum charge

C-rate has no beneficial effect on profitability (except for a very small region) because the charger has already hit the maximum power level. It is instead important to increase the battery specific energy to reduce the overall size of the aircraft and decrease the amount of energy required to fly the economic mission: this region is clearly defined by the horizontal gradient arrows and vertical isolines. As the $P_{\text{ch}}^{(\max)}$ increases (Figs. 9b and 9c), it appears a region of the design where it is beneficial to improve both ρ_E and $C_{\text{ch}}^{(\max)}$ due to their mutual effect on E_b^* . The small white strip on the far left side of the plots represents the design space region for which the aircraft cannot complete the sizing requirement at any weight below 12,500lb.

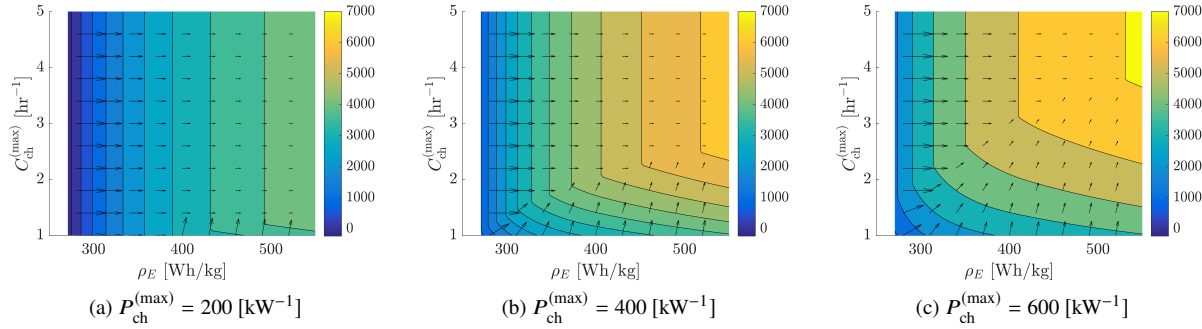


Fig. 9 $\Pi^{(\text{day})}$ for Lift-plus-Cruise configuration flying on the specified network for different values of $P_{\text{ch}}^{(\max)}$

Fig. 10 shows the contour of profitability with respect to the charger power and the battery specific energy at different maximum charge C-rates. Similarly to Fig. 9, increasing the specific energy of the battery always leads to an increase in profitability by reducing the optimal weight. In this regime, increasing the charger power has no effect on profitability because the maximum allowable charge C-rate is the constraint and does not allow the number of completed routes to increase. This region is clearly marked by the horizontal gradient markers and vertical isolines. At higher charge C-rates, it is beneficial to increase the specific energy and the charger power due to their influence on E_b^* . From a technology investment point of view, an increase in $P_{\text{ch}}^{(\max)}$ has almost zero benefit to the profitability for ρ_E values below 350 [Wh/kg] irrespective to the $C_{\text{ch}}^{(\max)}$ level. Considering that battery technology is currently well below the 350 [Wh/kg] level, the above simplified analysis suggests that there is almost zero benefit in pushing toward an increase in $P_{\text{ch}}^{(\max)}$.

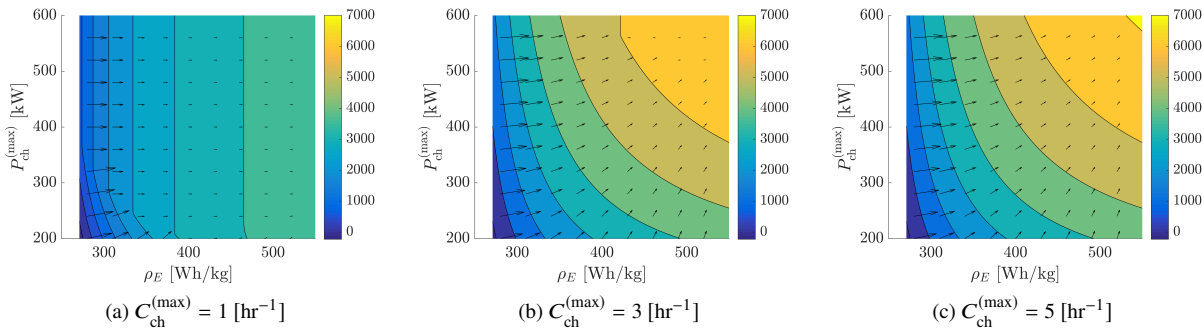


Fig. 10 $\Pi^{(\text{day})}$ for Lift-plus-Cruise configuration flying on the specified network for different values of $C_{\text{ch}}^{(\max)}$

Fig. 11 shows the same profitability contour plots in Fig. 9 stacked in a three dimensional space to make a comparison between the three aircraft configurations possible. As can be observed, based on this simplified performance model, the side-by-side configuration is the most profitable to fly the mission defined in Section II.C within the entire design space considered in this study. Fig. 12 shows that the optimal weight for profitability is primarily driven by the specific energy of the battery, and that the obtained optimal weights are close to the nominal values reported in Table 3. As expected, the side by side configuration has smaller optimal weights due to its relatively low ϕ_e and disk loading.

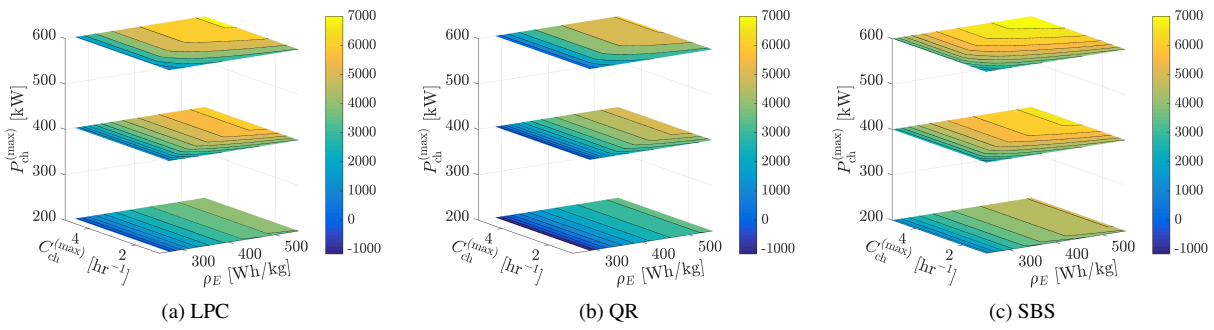


Fig. 11 $\Pi^{(\text{day})}$ for different aircraft configurations configuration flying the specified city network

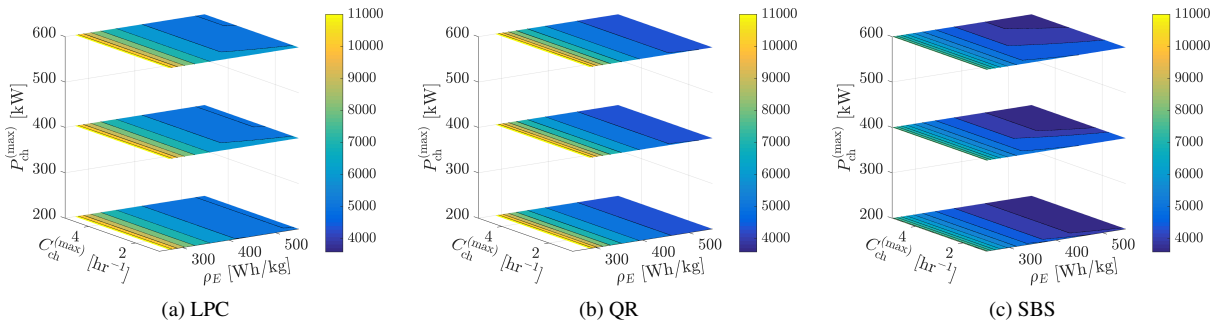


Fig. 12 $W^{(II)}$ for different aircraft configurations configuration flying the specified city network

VI. Conclusion

In this paper, we examined how range and battery technology factors such as specific energy and maximum C-ratings affect the sizing and performance of eVTOL aircraft operating in the context of UAM. This was done by first creating a simple “energy in a tank” battery model and economic model. The UAM network was defined by two ranges: the maximum range is the maximum distance the aircraft is sized to fly, the economical range is the demand-weighted mean mission distance. These pieces are brought together with a high level aircraft performance model flexible enough to compare the performance of aircraft as diverse as a quadcopter, side-by-side helicopter, and lift plus cruise. The aircraft model was then used to analytically determine the aircraft gross weight that maximizes both number of completed routes and a profitability index. The maximum number of completed routes is shown to correspond to a battery sized such that the limiting charge rate corresponds to both the maximum charger power and the maximum rate allowable C-rate. The aircraft weight that maximizes profit is either at or below this weight.

Finally, the model was used to perform sensitivity studies that explore the effect of aircraft weight and profitability with respect to changes of battery and charger technology parameters. These sensitivities can be used to determine which technology requires the most immediate improvement and how an aircraft should be designed to prepare for changes in technology. At a low battery specific energy, it is not necessary to increase the power of the charger or the charge C-rates. There is always a benefit to increasing the specific energy of the battery and once battery specific energy values increase, it will be important to increase the charge C-rate of the battery and the charger power as well.

References

- [1] Holden, J., and Goel, N., “Uber Elevate: Fast-Forwarding to a Future of On-Demand Urban Air Transportation,” Technical report, Uber Technologies, 2016. URL <https://www.uber.com/elevate.pdf>.

[2] Daskilewicz, M., German, B., Warren, M., Garrow, L. A., Boddupalli, S.-S., and Douthat, T. H., “Progress in Vertiport Placement and Estimating Aircraft Range Requirements for eVTOL Daily Commuting,” *2018 Aviation Technology, Integration, and Operations Conference*, 2018, p. 2884.

- [3] Hamilton, T. K., and German, B., "Airspeeds for Scheduled Electric Aircraft Operations," *17th AIAA Aviation Technology, Integration, and Operations Conference*, 2017, p. 3284.
- [4] Duffy, M. J., Wakayama, S. R., and Hupp, R., "A Study in Reducing the Cost of Vertical Flight with Electric Propulsion," *17th AIAA Aviation Technology, Integration, and Operations Conference*, American Institute of Aeronautics and Astronautics, Denver, Colorado, 2017. doi:10.2514/6.2017-3442, URL <https://arc.aiaa.org/doi/10.2514/6.2017-3442>.
- [5] Booz Allen Hamilton, "Urban Air Mobility (UAM) Market Study - Executive Briefing," , Oct. 2018.
- [6] Kohlman, L. W., and Patterson, M. D., "System-Level Urban Air Mobility Transportation Modeling and Determination of Energy-Related Constraints," *2018 Aviation Technology, Integration, and Operations Conference*, AIAA AVIATION Forum, American Institute of Aeronautics and Astronautics, 2018. doi:10.2514/6.2018-3677, URL <https://arc.aiaa.org/doi/10.2514/6.2018-3677>.
- [7] German, B., Daskilewicz, M., Hamilton, T. K., and Warren, M. M., "Cargo Delivery in by Passenger eVTOL Aircraft: A Case Study in the San Francisco Bay Area," *2018 AIAA Aerospace Sciences Meeting*, 2018, p. 2006.
- [8] Silva, C., Johnson, W., Antcliff, K., and Patterson, M., "VTOL Urban Air Mobility Concept Vehicles for Technology Developement," AIAA Aviation Forum, Atlanta, GA, 2018.
- [9] Clarke, S., "Flight Demonstrations and Capabilities," , Nov. 2016. URL https://www.nasa.gov/sites/default/files/atoms/files/sceptor_cdr_day_1_package.pdf.
- [10] Division, S. E. B., "Introduction of INR18650-30Q," , ????
- [11] "Panasonic Lithium Ion NCR18650," , ???? URL <https://engineering.tamu.edu/media/4247819/ds-battery-panasonic-18650ncr.pdf>.
- [12] Tesla, "Supercharger," , 2018. URL <https://www.tesla.com/supercharger>.
- [13] Jackson, L., "ABB powers e-mobility with launch of first 150-350 kW high power charger," , Oct. 2017. URL <http://www.abb.com/cawp/seitp202/c2ed43a8ef2e1de2c12581ae002d26b8.aspx>.